Physics of Fluids

A vortex identification method based on local fluid rotation

Cite as: Phys. Fluids **32**, 015104 (2020); https://doi.org/10.1063/1.5133815
Submitted: 04 November 2019 . Accepted: 18 December 2019 . Published Online: 08 January 2020

Shuling Tian (田书玲), Hao Fu (付豪), Jian Xia (夏健), and Yong Yang (杨勇)

ARTICLES YOU MAY BE INTERESTED IN

A vortex identification method based on local fluid rotation

Cite as: Phys. Fluids 32, 015104 (2020); doi: 10.1063/1.5133815
Submitted: 4 November 2019 • Accepted: 18 December 2019 •
Published Online: 8 January 2020

Shuling Tian (田书玲),[1,a)] Hao Fu (付豪),[1] Jian Xia (夏健),[1] and Yong Yang (杨勇)[2]

AFFILIATIONS

[1] Key Laboratory of Unsteady Aerodynamics and Flow Control, Ministry of Industry and Information Technology, Nanjing University of Aeronautics and Astronautics, Nanjing, Jiangsu 210016, China
[2] School of Engineering, Computer Science and Mathematics, West Texas A&M University, Canyon, Texas 79016, USA

Note: This paper is part of the Special Topic, Papers Selected from the 8th International Symposium on Physics of Fluids.
[a)] **Electronic mail:** shulingtian@nuaa.edu.cn

ABSTRACT

In this work, a vortex identification method is developed by analyzing the physical meaning of the local rotation of fluid elements. It is shown that a point is locally rotational when the velocity gradient tensor at the point has a pair of complex eigenvalues. The local rotation can be represented by a so called vortex vector. The direction of the vortex vector is defined as that of the local fluid rotation axis, which is parallel to the eigenvector of velocity gradient tensor corresponding to the real eigenvalue. The magnitude is evaluated as the twice of the minimum angular velocity around the point among all azimuth in the plane perpendicular to the vortex vector. Based on the local fluid rotation, a vortex is identified as a connected region where the vortex vector at each point is not equal to zero. The vortex identification method is validated by applying it to Reynolds-averaged Navier-Stokes data and direct numerical simulation data. The results reveal that the method can fully describe the complex structures of vortices.

I. INTRODUCTION

Vortices are ubiquitous in the fluid flows of nature and industry, and many detrimental effects may be induced by them, such as the destructiveness of a tornado, structural failure due to vortex-induced vibration, the drag induced by the action of the tip vortices, and the noise due to vortical structures formed along the turbulent boundary layers.[1–9] Many experimental techniques and numerical methods have been developed to investigate the formation and maintenance of vortical structures,[10–17] but there is a lack of a consensus on the vortex definition. A vortex is always featured as the rotation of fluid, and it can be easily recognized as a rotational region in which a multitude of material particles rotate around a common center,[18] but it is surprisingly difficult to give an unambiguous definition for the vortex.[19] In the classic aerodynamics, a vortex is always qualitatively identified as a connected region with relatively high concentration of vorticity or as a region where the closed or spiral streamlines can be created. This may be intuitively reasonable for the large scale vortical structures such as tornadoes.[1] However, the association between the regions of strong vorticity and the actual vortices can be rather weak in the three dimensional (3D) boundary layer flow.[20] Therefore, a vortex cannot be fully represented by a vorticity tube,[21] and the closed or spiral streamlines even cannot be generated in the boundary layer flow as they are highly related to the reference frame. Therefore, the definition of the vortex is still an open issue in fluid dynamics.[22,23]

In recent decades, many vortex identification methods were proposed, such as Q-method,[24] λ_2-method,[25] λ_{ci}-method,[26,27] Ω-method,[28] λ_ω-method,[29] and many others.[30–33] In these methods, a vortex is described by a scalar variable and is often visualized by the isosurface of these scalar variables. However, a vortex has both the direction and strength and these vortex identification methods cannot identify the rotational direction. To fully describe the vortex structure, a so called vortex vector was proposed in Ref. 34, in which the direction of the vortex vector is solved by using the Newton-iterative method. Although the method will converge rather fast if the initial guess is sufficiently close to the solution, a more efficient method is needed. In this study, the vortex identification method is further developed and a new means is used to solve the direction of the local fluid rotation.

The outline of the paper is as follows. Section II presents the physical meaning of local fluid rotation by analyzing the motion of the two-dimensional and three-dimensional fluid elements. Section III presents the vortex identification method based on the concept of local fluid rotation. In Sec. IV, the large-scale vortical structures behind a missile at a high induced angle and small-scale vortices in the late flow transition of plate plane boundary layer are visualized in different forms by applying the present vortex identification method. Finally, Sec. V concludes this work.

II. LOCAL FLUID ROTATION

The streamlines are often utilized to visualize the flow structures in the engineer problems, but this method does not satisfy the requirement of the Galilean invariant[25] as the form of the streamlines is highly related to the reference frame. However, as Robinson stated,[35] a vortex exists when instantaneous streamlines mapped onto a plane normal to the vortex core exhibit a roughly circular or spiral pattern, when viewed from a reference frame moving with the center of the vortex core. Therefore, we can identify a vortex by using the closed or spiral streamlines based on the local relative velocity. In this study, a point is considered to be locally rotational if the closed or spiral streamlines can be created in its neighborhood using the velocity relative to it. By using the concept of local fluid rotation, a vortex can be identified as a connected region in which every point is locally rotational. The local fluid rotation at a point will be analyzed in Subsections II A and II B.

A. Angular velocity of local fluid rotation

Consider a fluid element in a two-dimensional flow on the XY plane as shown in Fig. 1(a). When it translates along the streamline during a time increment Δt, it may also rotate and become distorted. The amount of rotation and distortion depends on the velocity field or the distribution of gradient tensor $\nabla \vec{V}_{XY}$. Sides AB and AC rotate because points B and C move differently from point A. The angular velocities of lines AB and AC are $\partial U/\partial Y$ and $\partial V/\partial X$, respectively. Side AB of the fluid element will have a clockwise rotation if $\partial U/\partial Y > 0$, a counterclockwise rotation if $\partial U/\partial Y < 0$, and no rotation if $\partial U/\partial Y = 0$. Side AC will have a counterclockwise rotation if $\partial V/\partial X > 0$, a clockwise rotation if $\partial Y/\partial X < 0$, and no rotation if $\partial V/\partial X = 0$. In the classic fluid dynamics, the angular velocity of the fluid element is defined as half of the vorticity that is equal to $\partial V/\partial X - \partial U/\partial Y$ in the two-dimensional flow. The angular velocity of the fluid element is defined as the average of the angular velocities of lines AB and AC. However, the fluid element may not have a rotation even if the angular velocity or vorticity is nonzero. For example, in the two dimensional (2D) laminar boundary layer flow, the vorticity is very large near the wall surface, but the closed or spiral streamlines based on the local relative velocity cannot be generated in it and no flow rotation or vortex is found. In this case, it is only considered as a pure shearing as shown in Fig. 1(b) in which $\partial V/\partial X = 0$. In addition, the closed or spiral streamlines cannot either be created when the sign of the angular velocity of line AB is different from that of line AC, as shown in Fig. 1(c) in which $\partial V/\partial X > 0$ and $\partial U/\partial Y > 0$. In this case, the element only has a distortion or deformation during the time increment Δt. Therefore, to describe the rotational motion of a fluid element with more obvious physical meaning, a new criterion is needed. In this paper, we propose that the element has a rotational motion only when the two sides AB and AC have the same rotational directions. As shown in Fig. 1(d) in which $\partial V/\partial X > 0$ and $\partial U/\partial Y < 0$, the element is said to be in a rotational motion.

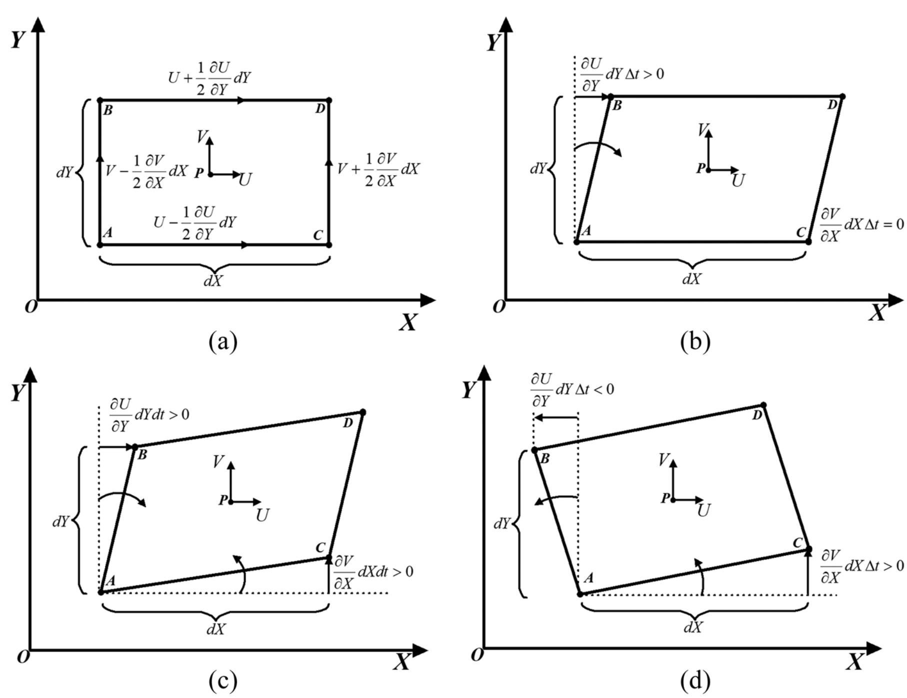

FIG. 1. Rotation and distortion of a fluid element in the two-dimensional flow on the XY plane: (a) the fluid element at time t; (b) the fluid element only has a pure shearing deformation if $\partial V/\partial X = 0$; (c) the fluid element has a irrotational deformation when ∂V/∂X and ∂U/∂Y have the same signs; and (d) the element has a rotational deformation when ∂V/∂X and ∂U/∂Y have different signs.

As shown in Fig. 1, $\partial V/\partial X$ and $\partial U/\partial Y$ can be thought as the angular velocities of sides AC and AB, respectively. However, they depend on the azimuth of the reference frame and their signs and the magnitudes will change when the reference frame rotates around Z axis. Therefore, the motion of the fluid element's sides cannot represent the rotation feature of the fluid at a point. The angular velocity around the point should be further investigated. Consider a point at which the velocity gradient tensor in the XY plane is

$$\nabla \vec{V}_{XY} = \begin{bmatrix} \frac{\partial U}{\partial X} & \frac{\partial U}{\partial Y} \\ \frac{\partial V}{\partial X} & \frac{\partial V}{\partial Y} \end{bmatrix}. \tag{1}$$

In addition, consider a line at an azimuth θ to OX axis as shown in Fig. 2. The angular velocity of the fluid along the line is

$$\begin{aligned} \omega_\theta &= \begin{bmatrix} -\sin\theta & \cos\theta \end{bmatrix} \begin{bmatrix} \frac{\partial U}{\partial X} & \frac{\partial U}{\partial Y} \\ \frac{\partial V}{\partial X} & \frac{\partial V}{\partial Y} \end{bmatrix} \begin{bmatrix} \cos\theta \\ \sin\theta \end{bmatrix} \\ &= \alpha \sin(2\theta + \varphi) + \beta, \end{aligned} \tag{2}$$

where

$$\alpha = 0.5\sqrt{\left(\frac{\partial V}{\partial Y} - \frac{\partial U}{\partial X}\right)^2 + \left(\frac{\partial V}{\partial X} + \frac{\partial U}{\partial Y}\right)^2}, \tag{3}$$

$$\beta = 0.5\left(\frac{\partial V}{\partial X} - \frac{\partial U}{\partial Y}\right), \tag{4}$$

and φ can be evaluated by

$$\tan\varphi = \left(\frac{\partial V}{\partial X} + \frac{\partial U}{\partial Y}\right) \Big/ \left(\frac{\partial V}{\partial Y} - \frac{\partial U}{\partial X}\right). \tag{5}$$

If $\alpha^2 < \beta^2$, the direction of angular velocity is invariant and a closed or spiral streamline can be generated. As stated above, the fluid at the point is locally rotational. To show the concept of local fluid rotation more clearly, the characters of rotation are investigated at two points in a two-dimensional flow of XY plane. The velocity gradient tensors at these two points are

$$\nabla \vec{V}_{XY}|_1 = \begin{bmatrix} 0.08 & -0.3 \\ 0.16 & -0.05 \end{bmatrix}$$

and

$$\nabla \vec{V}_{XY}|_2 = \begin{bmatrix} -0.25 & -0.025 \\ 0.125 & 0.150 \end{bmatrix}.$$

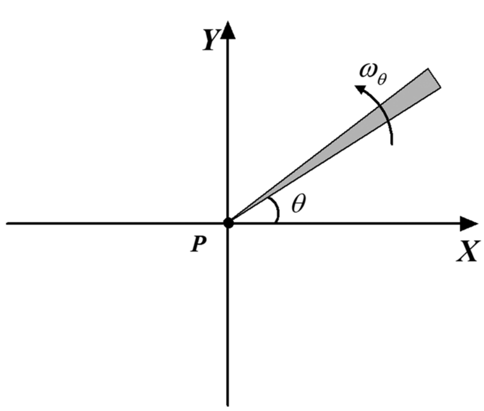

FIG. 2. The local angular velocity of the fluid along the line at an azimuth θ to X axis.

The distributions of the angular velocity and relative velocity component in the tangential direction around the points are shown in Fig. 3. The fluid has an invariant direction rotation (counterclockwise) around point 1 (as $\alpha^2 < \beta^2$ for $\nabla \vec{V}_{XY}|_1$) and the closed or spiral streamlines can be created using the velocity relative to point 1 [see Figs. 3(a) and 3(b)]. However, they cannot be generated at point as the rotation direction is variant with the azimuth θ around it [see Figs. 3(c) and 3(d)] (as $\alpha^2 < \beta^2$ for $\nabla \vec{V}_{XY}|_2$), which means that this point is not locally rotational.

Different from the rotation of rigid body which has the same angular velocity for each point, the angular velocity of fluid, even if at the same point, varies with the azimuthal angle. In this study, we use the minimum value of Eq. (2) as the angular velocity of local rotation and

$$\omega_{rot} = \begin{cases} \beta - \alpha, & if\ \beta > 0\ and\ \alpha^2 < \beta^2 \\ \beta + \alpha, & if\ \beta < 0\ and\ \alpha^2 < \beta^2 \\ 0, & if\ \alpha^2 < \beta^2 \end{cases}. \tag{6}$$

For the 2D flow, the direction of angular velocity of a fluid-rotational point is perpendicular to the 2D plane, and so we can have the following conclusion:

(1) If $\omega_{rot} > 0$, the local fluid-rotation is counterclockwise.
(2) If $\omega_{rot} < 0$, the local fluid-rotation is clockwise.
(3) If $\omega_{rot} = 0$, the point is not fluid-rotational.

It can be shown that that $\nabla \vec{V}_{XY}$ has two complex eigenvalues if $\alpha^2 < \beta^2$. This means that a point is locally rotational in a two-dimensional flow if the velocity gradient tensor at this point has two complex eigenvalues.

As shown in Fig. 4, if the signs of angular velocity at all points are the same in a connected region, the closed or spiral streamlines based on the local relative velocity can be created at any point. A 2D vortex can be recognized in this region. Therefore, we can identity a vortex in a 2D flow by using the eigenvalues of velocity gradient tensor and local angular velocity.

B. Direction of local fluid rotation

In 2D flows, the direction of rotation axis is predetermined, which is normal to the 2D plane, but it is not easy for the 3D flows. So, how to find the rotation axis for a fluid element in a 3D flow is the main objective of this subsection. According to its definition, a rotation axis does not rotate. Therefore, using this character, the direction of rotation axis at a point can be found by analyzing the motion of the 3D fluid element. The fluid element at a point can be centered in any reference frame, but there should be a frame in which the analysis can be carried out most conveniently. In this study, we will analyze the motion of a fluid element in a special reference frame, which can be transformed from the general reference frame.

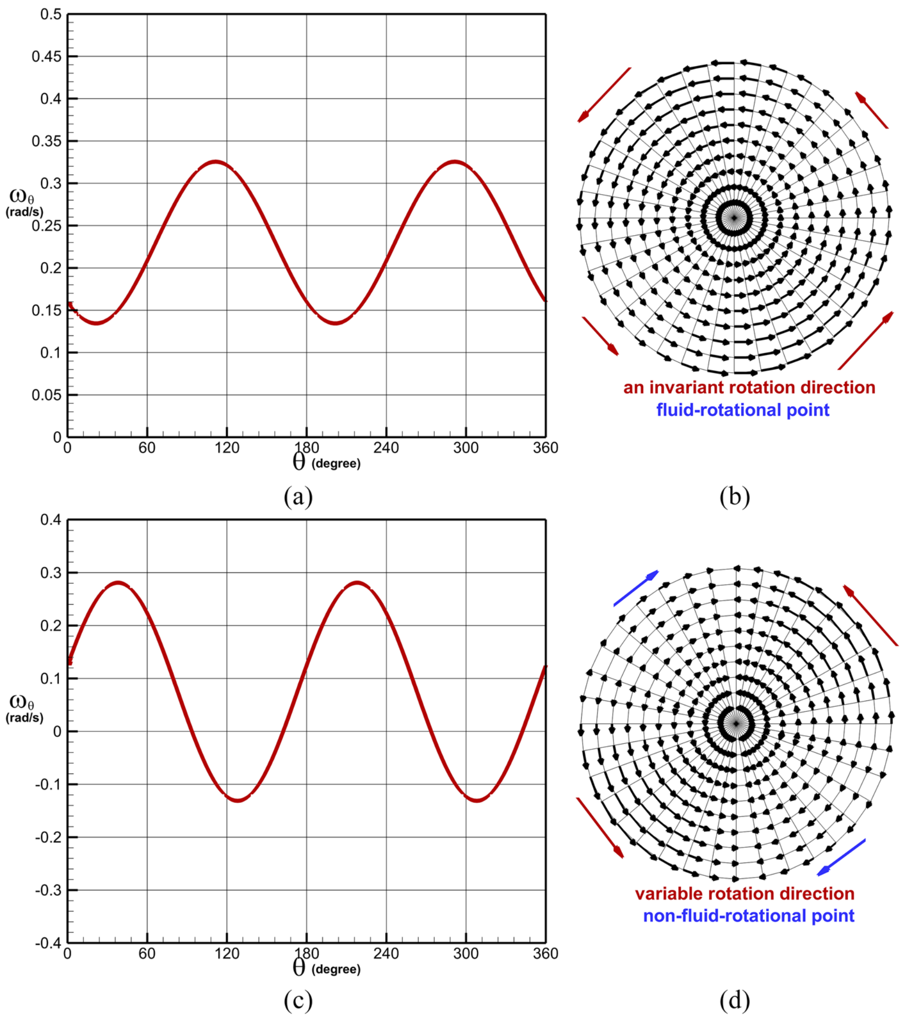

FIG. 3. Rotation character of fluid around two points: (a) angular velocity distribution of fluid around the first point; (b) distribution of velocity components in tangential direction around the first point; (c) angular velocity distribution of fluid around the second point; and (d) distribution of velocity components in tangential direction around the second point.

Consider a point P in the general reference frame xyz and assume that the vector $\vec{r}_{xyz} = [r_x, r_y, r_z]^T$ is its rotation axis which does not have a rotational velocity. If the fluid element is located in the frame xyz in which $\vec{r}_{xyz}$ is not parallel to any coordination axis, it may not be easy to analyze the motion of the fluid element. To conveniently analyze the rotation, the fluid element can be considered in a new reference frame XYZ in which the fluid-rotational axis vector $\vec{r}_{XYZ}$ is parallel to the axis OZ. Therefore, there is a transformation matrix $\boldsymbol{Q}$ from frame xyz to frame XYZ, which can make the following formula valid:

$$\vec{r}_{XYZ} = \boldsymbol{Q}\vec{r}_{xyz}, \tag{7}$$

where $\vec{r}_{XYZ} = [0, 0, 1]^T$. Obviously, $\boldsymbol{Q}$ is the function of $\vec{r}_{xyz}$ and can be written as[34]

$$\boldsymbol{Q} = \begin{bmatrix} \dfrac{r_y^2 + r_z^2 + r_z}{1 + r_z} & -\dfrac{r_x r_y}{1 + r_z} & -r_x \\ -\dfrac{r_x r_y}{1 + r_z} & \dfrac{r_x^2 + r_z^2 + r_z}{1 + r_z} & -r_y \\ r_x & r_y & r_z \end{bmatrix}. \tag{8}$$

With the transformation matrix $\boldsymbol{Q}$, the velocity gradient tensor $\nabla\vec{V}$ in the reference frame XYZ can be given as

$$\nabla\vec{V} = \boldsymbol{Q}\nabla\vec{v}\boldsymbol{Q}^{-1}, \tag{9}$$

where $\nabla\vec{v}$ is the velocity gradient tensor in the general reference frame xyz.

Consider the fluid element in the reference frame XYZ shown in Fig. 5(a). The rotation and distortion of fluid element $ABCD-A'B'C'D'$ depends solely on $\nabla\vec{V}$. As $\vec{r}_{XYZ} = [0, 0, 1]^T$ is the local rotation axis, the direction of sides AB, DC, $A'B'$, $D'C'$ must remain the same during the motion of the fluid element. However, if $\partial U/\partial Z \neq 0$ or $\partial V/\partial Z \neq 0$, these sides must rotate around an axis parallel to the XOY plane. For example, the sides AB, DC, $A'B'$, $D'C'$ will have a clockwise rotation in the plane parallel to YOZ plane if $\partial U/\partial Z < 0$ as shown in Fig. 5(b), and they will have a counterclockwise rotation around an axis parallel to OX axis if $\partial V/\partial Z > 0$ as shown in Fig. 5(c), which are a contradiction to the assumption that the local rotation axis is parallel to OZ axis. As shown in Fig. 5(d), if $\partial W/\partial X \neq 0$, the sides AA', BB', CC', DD' have a rotation, but it

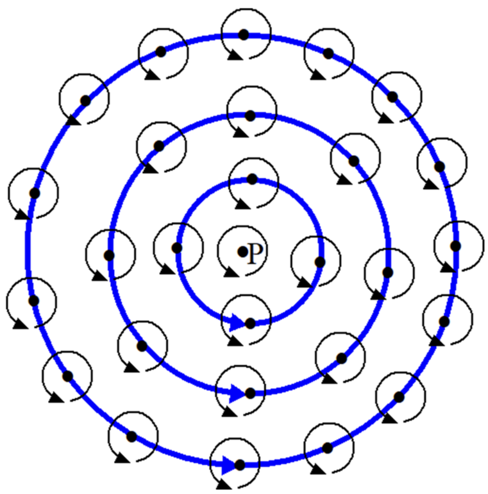

FIG. 4. The closed or spiral streamlines created in a connected region in which α^2 is smaller than β^2 and ω_{rot} keep the same sign.

cannot change the direction of the sides AB, DC, $A'B'$, $D'C'$. In the same way, $\partial W/\partial Y$, $\partial V/\partial X$, $\partial U/\partial Y$, $\partial U/\partial X$, $\partial V/\partial Y$, $\partial W/\partial Z$ cannot cause a rotation of sides AB, DC, $A'B'$, $D'C'$. Based on the above analysis, if the direction of rotation axis at the point is parallel to OZ axis, the velocity gradient tensor $\nabla\vec{\boldsymbol{V}}$ in reference frame XYZ must have a form as

$$\nabla\vec{\boldsymbol{V}} = \begin{bmatrix} \frac{\partial U}{\partial X} & \frac{\partial U}{\partial Y} & 0 \\ \frac{\partial V}{\partial X} & \frac{\partial V}{\partial Y} & 0 \\ \frac{\partial W}{\partial X} & \frac{\partial W}{\partial Y} & \frac{\partial W}{\partial Z} \end{bmatrix}. \tag{10}$$

Based on the Schur decomposition theory,[36] for the velocity gradient tensor $\nabla\vec{\boldsymbol{v}}$ in a general reference frame, there must be an orthogonal matrix $\boldsymbol{Q}$ which can make $\nabla\vec{\boldsymbol{V}}$ be a blocks-triangular matrix such as Eq. (10).[34,37] By solving the nonlinear algebraic equations $\partial U/\partial Z = 0$, $\partial V/\partial Z = 0$ and $r_x^2 + r_y^2 + r_z^2 = 1$, the local rotation axis vector $\vec{\boldsymbol{r}}_{xyz}$ in the general reference frame can be found. In Ref. 34, the equations are solved by using the Newton-iterative method. Though Newton-iterative method is very efficient if the initial guess is sufficiently close to the solution, an explicit method is still needed.

By analyzing Eq. (10), it can be found that

$$\nabla\vec{\boldsymbol{V}}\vec{\boldsymbol{r}}_{XYZ} = \frac{\partial W}{\partial Z}\vec{\boldsymbol{r}}_{XYZ}, \tag{11}$$

where $\vec{\boldsymbol{r}}_{XYZ} = [0,0,1]^T$. Equation (11) implies that the vector of local fluid rotation axis $\vec{\boldsymbol{r}}_{XYZ}$ is the eigenvector of velocity gradient tensor. Because $\partial W/\partial Z$ is the derivative of the velocity, it must be a real number. Therefore, the local rotation axis must be parallel to the eigenvector corresponding to the real eigenvalue of velocity gradient tensor in the fame XYZ.[38] As $\nabla\vec{\boldsymbol{V}}$ and

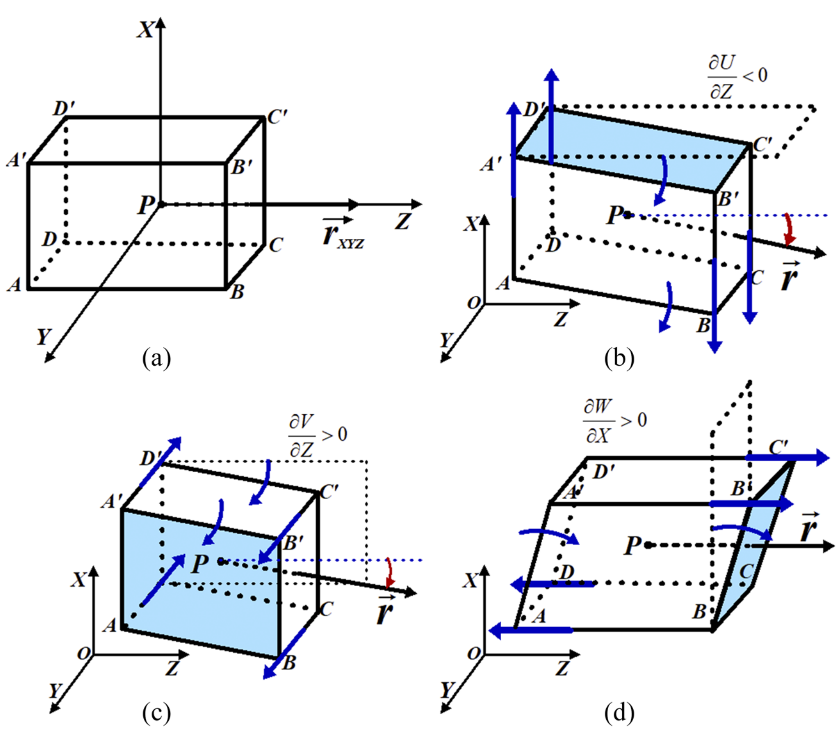

FIG. 5. Rotation and distortion of a fluid element in 3D: (a) fluid element at time t in a transformed reference frame XYZ; (b) $\partial U/\partial Z \neq 0$ causes a rotation around Y axis to the surface ABCD, A′B′C′D′ and to vector $\vec{r}_{xyz}$; (c) $\partial V/\partial Z \neq 0$ causes a rotation around X axis to the surface $ABB'A'$, $DCC'D'$ and vector $\vec{r}_{xyz}$; and (d) $\partial W/\partial X \neq 0$ does not change the direction of vector $\vec{r}_{xyz}$ and only causes shearing in Z direction.

$\nabla\vec{v}$ are similar, the local rotation axis in the general reference frame *xyz* is also parallel to the eigenvector of the velocity gradient tensor $\nabla\vec{v}$ corresponding to the real eigenvalue. Therefore, we have

$$\nabla\vec{v}\,\vec{r}_{xyz} = \lambda\vec{r}_{xyz}, \tag{12}$$

where λ is the real eigenvalue and $\vec{r}_{xyz}$ is its eigenvector. As velocity gradient tensor $\nabla\vec{v}$ is a 3 × 3 matrix, its eigenvalues and eigenvectors can be solved utilizing a set of explicit formulas.

However, the form of velocity gradient tensor as shown in Eq. (10) in a reference frame by no means implies that there is a local fluid rotation around *OZ* axis. It only shows that the fluid has no rotation around the axes *OX* and *OY*, or, in other words, that the fluid only has shear or/and deformation in the X and Y directions. Therefore, after we find the rotation axis, we should further determine if there is local fluid rotation around the axis aligned with $\vec{r}_{xyz}$ at point P, which can be distinguished by analyzing the distributions of velocity derivatives in the normal plane *XY* of vector $\vec{r}_{xyz}$ using the method proposed in Subsection II A. The velocity gradient tensor in the special reference frame *XYZ* can be obtained by using Eq. (9). According to the conclusion that a point in a 2D flow is locally rotational if the velocity gradient tensor in the flow plane has two complex eigenvalues, it can be drawn that a point in a 3D flow is locally rotational if the velocity gradient tensor has one real and two complex eigenvalue and the local rotation axis is parallel to the eigenvector corresponding to the real eigenvalue.

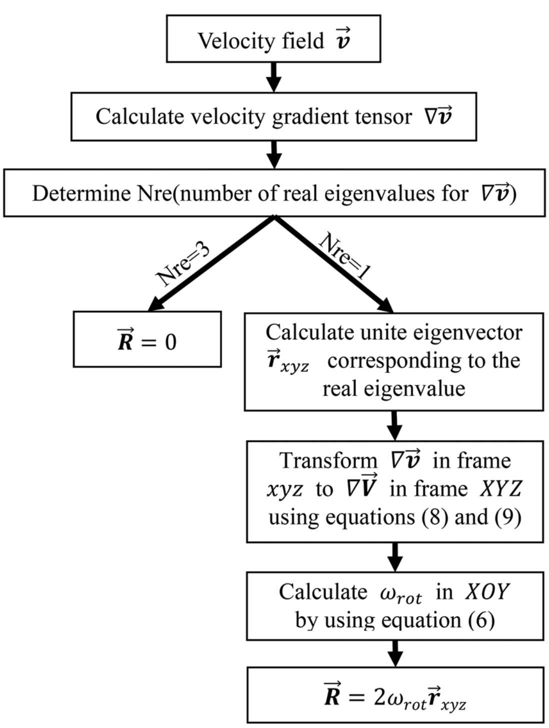

FIG. 6. Flowchart of calculating vortex vector in the velocity field.

III. VORTEX IDENTIFICATION BASED ON LOCAL FLUID ROTATION

As vortex is featured as the rotation of fluid, it is very logical to identify a vortex using the concept of local rotation. With the definitions of the angular velocity and rotation axis of local rotation, a new vector can be defined to describe the local rotation. The new vector, which is called vortex vector and written as $\vec{R}$ in Ref. 34, can be used to identify vortex. Similar to the definition of vorticity which is twice the average angular velocity, the magnitude of vortex vector is set as twice the velocity of local rotation. The direction of vortex vector is that of the rotation axis or the local fluid rotation. Therefore, it is written as

$$\vec{R} = 2\omega_{rot}\vec{r}_{xyz}. \tag{13}$$

According to Eqs. (6) and (13), it can be seen that $\vec{R}$ is a part of the vorticity component in the direction of local fluid rotation. $\vec{R} \neq 0$ when the velocity gradient tensor has two complex eigenvalues and one real eigenvalue. The direction of $\vec{R}$ is parallel to the eigenvector corresponding to the real eigenvalue. However, if the velocity gradient tensor at a point has three real eigenvalue, the point is not locally rotational and the vortex vector is zero. According to the definition and the analysis in Sec. II, the vortex vector can be evaluated by the following steps as shown in Fig. 6:

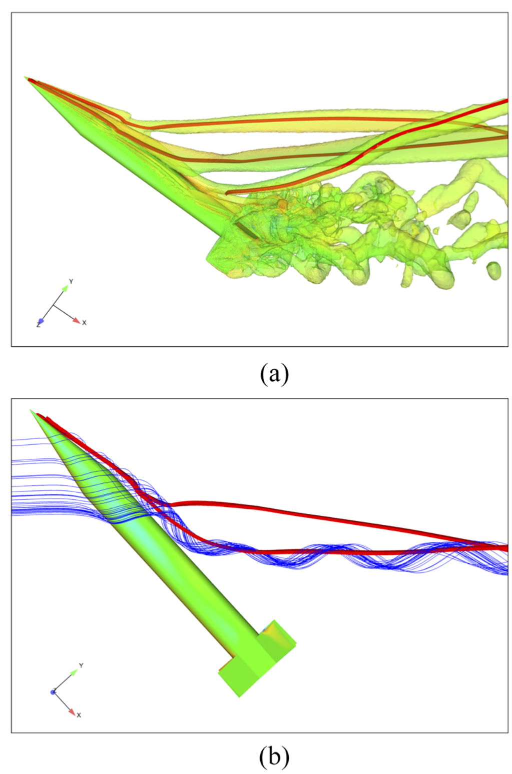

FIG. 7. The vortex structures in the flow field around a missile model in a high induced angle: (a) the vortex structures visualized by isosurface of the magnitude of vortex vector and vortex lines; (b) the spiral streamlines around a vortex line.

(1) Calculate the velocity gradient tensor in the general reference frame *xyz*.
(2) Calculate the eigenvalues of the velocity gradient tensor $\nabla\vec{v}$. If $\nabla\vec{v}$ has three real eigenvalues, the point is not locally rotational and $\vec{R} = 0$; if it has two complex eigenvalues and one real eigenvalue, go to step (3).
(3) Calculate the unit eigenvector $\vec{r}_{xyz}$ corresponding to the real eigenvalue and set $\vec{r}_{xyz}$ as the local rotation axis.
(4) Using Eqs. (8) and (9), transform the velocity gradient tensor from the reference frame *xyz* to the special reference frame *XYZ* in which the rotation axis is parallel to *OZ* axis.
(5) Obtain $\nabla\vec{V}_{XY}$ in Eq. (1) by deleting the 3rd row and 3rd column of $\nabla\vec{V}$ in Eq. (10) and calculate the angular velocity ω_{rot} of local fluid rotation in *XOY* by using Eq. (6) and set $\vec{R}$ as $2\omega_{rot}\vec{r}_{xyz}$ based on Eq. (13).

After the distribution of vortex vector in the flow field is obtained, a vortex can be identified as a connected region in which vortex vector is nonzero at each point. As the vortex vector is a vector quantity, a vortex can not only be visualized as the isosurface of the magnitude of vortex vector but also be shown by vortex line which is a curve to which the vortex vector is tangent at any point.

IV. VALIDATION OF THE VORTEX IDENTIFICATION METHOD

Vortical structures play an important role in many problems, from the large scale of hurricanes to the small size of turbulence. An accurate vortex identification method can reduce the confusions in understanding the mechanism of the evolution and interaction of vortical structures in complex vortical flows. The vortex identification method based on the local fluid rotation can not only give the rotation strength of a vortex but also show the rotation direction. In addition, the present developed method has an explicit form and the evaluation of vortex vector is more efficient. To validate the method, the vortex structures in two cases are investigated: one is the Reynolds-averaged Navier-Stokes (RANS) data of a missile model at high induced angle; the other is the direct numerical simulation (DNS) data of three-dimensional boundary layer flow transition.

A. Flow about a missile at high induced angle

High induced angle aerodynamics has been a key element in aircraft design.[39] It is always characterized by small- and large-scale, static and dynamic flow interactions that may include mixed regions

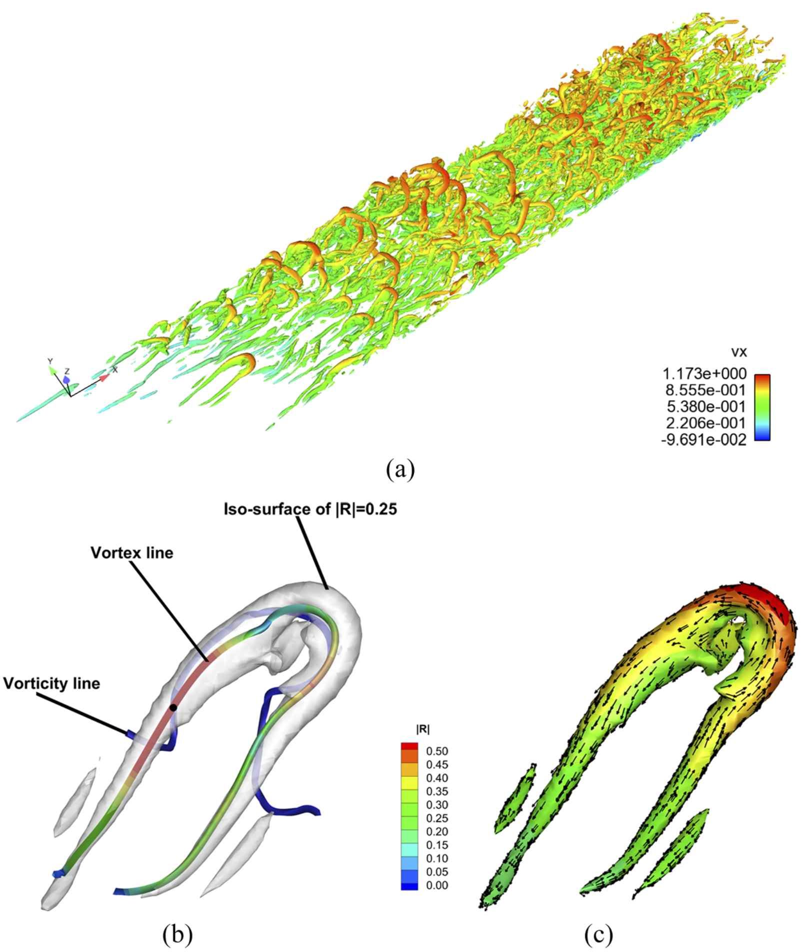

FIG. 8. The vortical structures in laminar-turbulence flow transition visualized by vortex vector (a) the process of vortical structures "build up;" (b) the isosurface and the vortex line of a hairpin vortex; and (c) the vector of the vortex vector which is aligned with the vortex core.

of attached flow, unorganized separated flow, and vortex flow. These interactions are unsteady and frequently strong enough to affect the pressure distributions not only on the missile body but also on the tail wings. As a result, the side force and hence a yawing moment are produced, which can cause the uncommanded motion of the aircraft. The control of the forebody vortex is thought as one of the most effective means to solve the high induced angle problem. Therefore, fully understanding the vortex structure in this problem is very helpful to design the controller. The flow field around a missile model at a high induced angle is simulated by using a RANS solver. As shown in Fig. 7(a), the asymmetric vortices behind the missile model are visualized by the isosurface of the magnitude of vortex vector. It can be seen that the large-scale vortex structures are clearly captured. To further show the ability of the present vortex identification method, the vortex lines are created using vortex vector indicated in Fig. 7(a). All the vortex cores presented by the isosurface are aligned with the vortex lines. This reveals that the vortex identification method provides a new means to show the complex vortex structures. When the streamlines are created near a vortex, they develop forward in a spiral form around the vortex line, as shown in Fig. 7(b), which implies that the global rotation feature of a vortex can be described by the local fluid rotation. The results show that the vortex identification method based on local fluid rotation can fully capture the large-scale vortex structures from the RANS data.

B. Plate plane boundary-layer flow transition

Boundary-layer transition to turbulence is one of very basic flow problems and experimental and numerical studies of wall-bounded flows reveal the ubiquitous presence of flow structures.[6,35,40,41] Compared to the vortex structures of the RANS data shown in Subsection IV A, the scale of the vortex structures in the boundary layer flow is very small. In order to verify the ability of the present vortex identification method in the application of the complex small-scale vortex structures, the DNS data of late boundary layer flow transition is used.

The transition of boundary layer flow is a process of vortex "buildup" as indicated in Fig. 8(a) which is visualized by the isosurface of $\left|\vec{\boldsymbol{R}}\right| = 0.25$. The small-scale vortex structures such as Λ-shaped vortex and hairpin vortex can be clearly observed in the process. Different from other scalar vortex identification method, the vortex can be plotted as vortex lines based on the vortex vector. As shown in Fig. 8(b), a hairpin vortex at the leading of Fig. 8(a) is described as a vortex line which aligned well with the cores of the vortex. However, the structure of the vorticity line which is created through the same point is different from that of the hairpin vortex core. This is because the vortex vector is the rotation part of the vorticity. Furthermore, Fig. 8(c) shows that the vector distribution of vortex vector on the surface of the hairpin vortex is highly consistent with the core of the vortex.

V. CONCLUSIONS

A vortex identification method based on the concept of local fluid rotation which was first proposed in Ref. 34 is further developed in this paper. By analyzing the motion of the two- and three-dimensional fluid elements, it is found that a point is locally rotational if the velocity gradient tensor has a pair of complex eigenvalues and one real eigenvalues. The direction of local fluid rotation is parallel to the eigenvector corresponding to the real eigenvector and the magnitude of rotational velocity is the twice of the minimum angular velocity of fluid around the point among all azimuth in the plane perpendicular to rotation axis. With these conclusions, vortex vector, which is used to describe the local fluid rotation, can be calculated with explicit formulas. Compared to the Newton-iterative method used in Ref. 34, the efficiency is greatly improved. Applications to the RANS data and DNS data show that the method can not only visualize the large-scale complex vortex structures such as the forebody vortex behind a missile but also capture the small-scale vortex structures in the boundary layer flow. In addition to be visualized as the isosurface, a vortex can be visualized as the vortex lines. Unlike the isosurface, the vortex line is not related to the threshold and it can avoid misunderstanding in recognizing vortex structures. Therefore, the present vortex identification method provides a new means to quantitatively investigate the physics of the generation and sustenance of vortex structures.

ACKNOWLEDGMENTS

The work was financially supported by the National Numerical Windtunnel (Grant No. NNW2019ZT7-B31). This research was also supported in part by the Department of Mathematics of University of Texas at Arlington and the Priority Academic Program Development of Jiangsu Higher Education Institutions.

REFERENCES

[1] M. Karami, H. Hangan, L. Carassale, and H. Peerhossaini, "Coherent structures in tornado-like vortices," Phys. Fluids **31**, 085118 (2019).
[2] M. Wang and P. Moin, "Computation of trailing-edge flow and noise using large-eddy simulation," AIAA J. **38**, 2201–2209 (2000).
[3] J. H. M. Ribeiro and W. R. Wolf, "Identification of coherent structures in the flow past a NACA0012 airfoil via proper orthogonal decomposition," Phys. Fluids **29**, 085104 (2017).
[4] T. Hiejima, "Streamwise vortex breakdown in supersonic flows," Phys. Fluids **29**, 054102 (2017).
[5] A. Sareen, J. Zhao, D. L. Jacono, J. Sheridan, K. Hourigan, and M. C. Thompson, "Vortex-induced vibration of a rotating sphere," J. Fluid Mech. **837**, 258–292 (2018).
[6] C. Lee and X. Jiang, "Flow structures in transitional and turbulent boundary layers," Phys. Fluids **31**, 111301 (2019).
[7] H. C. Ghimire and S. C. C. Bailey, "An experimental investigation of wing-tip vortex decay in turbulence," Phys. Fluids **29**, 037108 (2017).
[8] S. Nadeem, R. U. Haq, and C. Lee, "MHD boundary layer flow over an unsteady shrinking sheet: Analytical and numerical approach," J. Braz. Soc. Mech. Sci. Eng. **37**, 1339–1346 (2015).
[9] J. Jimenez, "Coherent structures in wall-bounded turbulence," J. Fluid Mech. **842**, 513–531 (2018).
[10] A. Limone, D. R. Hatch, C. B. Forest, and F. Jenko, "Identification of vortexes obstructing the dynamo mechanism in laboratory experiments," Phys. Fluids **25**, 066603 (2013).
[11] J. Zhang, H. Tian, Z. Yao, P. Hao, and N. Jiang, "Evolutions of hairpin vortexes over a superhydrophobic surface in turbulent boundary layer flow," Phys. Fluids **28**, 095106 (2016).
[12] H. Jiang and B. Ma, "Experiments on self-sustained oscillations of leeward vortices over a hemisphere cylinder," Phys. Fluids **31**, 097109 (2019).
[13] F. Qu, D. Sun, J. Bai, and C. Yan, "A genuinely two-dimensional Riemann solver for compressible flows in curvilinear coordinates," J. Comput. Phys. **386**, 47–63 (2019).

[14]R. U. Haq, Z. H. Khan, W. A. Khan, and I. A. Shah, "Viscous dissipation effects in water driven carbon nanotubes along a stream wise and cross flow direction," Int. J. Chem. React. Eng. **15**(1), 93–101 (2017).
[15]R. U. Haq, F. A. Soomro, Z. H. Khan, and Q. M. A. Mdallal, "Numerical study of streamwise and cross flow in the presence of heat and mass transfer," Eur. Phys. J. Plus **132**, 214 (2017).
[16]F. Qu, J. Chen, D. Sun, J. Bai, and C. Yan, "A new all-speed flux scheme for the Euler equations," Comput. Math. Appl. **77**, 1216–1231 (2019).
[17]O. Marxen, M. Lang, and U. Rist, "Vortex formation and vortex breakup in a laminar separation bubble," J. Fluid Mech. **728**, 58–90 (2013).
[18]H. J. Lugt, "The dilemma of defining a vortex," in *Recent Developments in Theoretical and Experimental Fluid Mechanics*, edited by K. G. Roesner, U. Mller, and B. Schmidt (Springer, 1979), pp. 309–321.
[19]P. Chakraborty, S. Balachandar, and R. J. Adrain, "On the relationships between local vortex identification schemes," J. Fluid Mech. **535**, 189–214 (2005).
[20]S. K. Robinson, S. J. Kline, and P. R. Spalart, "A review of quasi-coherent structures in a numerically simulated turbulent boundary layer," NASA Technical Report No. 102191, 1989.
[21]Y. Wang, Y. Yang, and C. Liu, "DNS study on vortex and vorticity in late boundary layer transition," Commun. Comput. Phys. **22**, 441 (2017).
[22]J. Wu, H. Ma, and M. Zhou, *Vorticity and Vortex Dynamics* (Springer, 2006).
[23]J. Wu, A. Xiong, and Y. Yang, "Axial stretching and vortex definition," Phys. Fluids **17**, 038108 (2005).
[24]J. C. Hunt, A. A. Wray, and P. Moin, "Eddies, streams, and convergence zones in turbulent flows," in *Proceedings of the Summer Program* (Center for Turbulence Research, 1988), p. 193.
[25]J. Jeong and F. Hussain, "On the identification of a vortex," J. Fluid Mech. **285**, 69 (1995).
[26]C. Berdahl and D. Thompson, "Eduction of swirling structure using the velocity gradient tensor," AIAA J. **31**, 97 (1993).
[27]J. Zhou, R. J. Adrian, S. Balachandar, and T. M. Kendall, "Mechanisms for generating coherent packets of hairpin vortices in channel flow," J. Fluid Mech. **387**, 353 (1999).
[28]C. Liu, Y. Wang, Y. Yang, and Z. Duan, "New omega vortex identification method," Sci. China: Phys., Mech. Astron. **59**, 1 (2016).
[29]J. H. Elsas and L. Moriconi, "Vortex identification from local properties of the vorticity field," Phys. Fluids **29**, 015101 (2017).
[30]V. Kolář, J. Šístek, F. Cirak, and P. Moses, "Average corotation of line segments near a point and vortex identification," AIAA J. **51**, 2678 (2013).
[31]H. Chen, Z. Wang, L. Zhu, and J. Wang, "Evaluation of vortex identification methods based on two- and three-dimensional swirling strengths," Phys. Fluids **30**, 125102 (2018).
[32]B. P. Epps, "Review of vortex identification methods," AIAA Paper 2017-0989, 2017.
[33]Y. Zhang, X. Qiu, F. Chen, K. Liu, X. Dong, and C. Liu, "A selected review of vortex identification methods with applications," J. Hydrodyn. **30**(5), 767–779 (2018).
[34]S. Tian, Y. Gao, X. Dong, and C. Liu, "Definitions of vortex vector and vortex," J. Fluid Mech. **849**, 312–339 (2018).
[35]S. K. Robinson, "Coherent motions in the turbulent boundary layer," Annu. Rev. Fluid Mech. **23**, 601–639 (1991).
[36]J. E. Gentle, *Numerical Linear Algebra for Applications in Statistics* (Springer, 1998).
[37]C. Liu, Y. Gao, S. Tian, and X. Dong, "Rortex—A new vortex vector definition and vorticity tensor and vector decompositions," Phys. Fluids **30**, 035103 (2018).
[38]Y. Gao and C. Liu, "Rortex and comparison with eigenvalue-based vortex identification criteria," Phys. Fluids **30**(8), 85107 (2018).
[39]G. E. Erickson, "High angle of attack aerodynamics," Annu. Rev. Fluid Mech. **27**, 45–88 (1995).
[40]R. J. Adrian, "Hairpin vortex organization in wall turbulence," Phys. Fluids **19**, 041301 (2007).
[41]H. Dong, T. Xia, L. Chen, S. Liu, Y. D. Cui, B. C. Khoo, and A. Zhao, "Study on flow separation and transition of the airfoil in low Reynolds number," Phys. Fluids **31**, 103601 (2019).